



Habitat suitability of Pacific saury (*Cololabis saira*) based on a yield-density model and weighted analysis



Chuanxiang Hua^{a,b,*}, Fei Li^a, Qingcheng Zhu^{a,b}, Guoping Zhu^{a,b}, Lingwen Meng^a

^a College of Marine Sciences, Shanghai Ocean University, Shanghai, 201306, China

^b National Engineering Research Center for Oceanic Fisheries, Shanghai, 201306, China

ARTICLE INFO

Handled by A.E. Punt

Keywords:

Habitat suitability index
Yield-density model
Weighted analysis
Oceanographic variation
Pacific saury

ABSTRACT

The Pacific saury (*Cololabis saira*) supports one of the most important pelagic fisheries in the Northwestern Pacific Ocean. However, changing oceanographic conditions could result in difficulties in predicting fishing grounds and fishery management. We combined a yield-density model and weighted statistical analysis to develop a habitat suitability index (*HSI*) model to identify the relationship between oceanographic variables and potential habitat. This approach was applied to fishing data from the Chinese saury fishery during the main fishing season (June–November) from 2013 to 2015. The oceanographic variables considered included sea surface temperature (SST), horizontal sea surface temperature gradient (SSTG) and sea surface height (SSH). The *HSI* model was validated using fishery and oceanographic data for 2016. This study indicated that (1) the yield-density model can be reliably used to fit a curvilinear relation between the suitability index (SI) and SST, SSTG, and SSH, and the optimal habitat conditions for the three variables were obtained; (2) weighted analysis-based boosted regression trees revealed that SSTG had the most important influence on SI each month, followed by SST and SSH; and (3) approximately 70% of the fishing effort occurred in the areas where *HSI* > 0.5 in each month. Results of this study could help to further understand the effects of oceanographic conditions on habitat distribution and provide a way to forecast saury fishing grounds.

1. Introduction

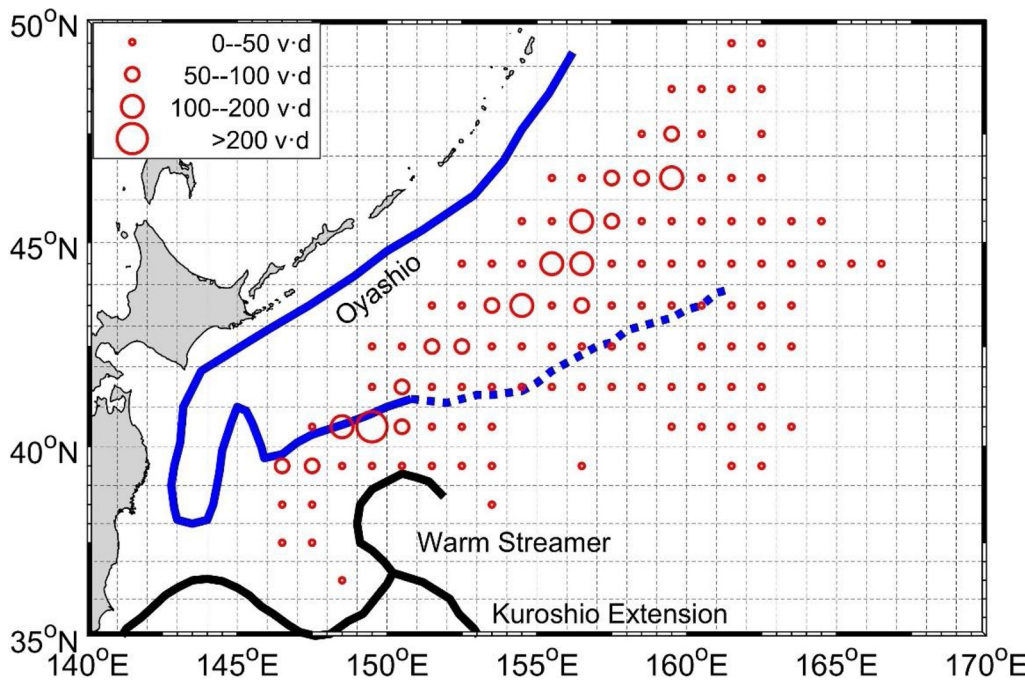
The Pacific saury, *Cololabis saira* (hereafter saury), is widely distributed in international waters, ranging from subarctic to subtropical regions throughout the Northwestern Pacific Ocean (Matsumiya and Tanaka, 1976). Following a long and large-scale migratory route, saury experiences extremely complicated oceanographic conditions as it passes northwards through the Kuroshio-Oyashio Transition Zone (TZ) in summer and then returns south to the coastal waters of Japan in winter (Fukushima, 1979; Gong, 1984). During migration, saury are mainly caught by countries and regions such as Japan, China, Chinese Taipei, Russia, South Korea and Vanuatu, and Chinese fishing vessels are mainly located east of the Hokkaido and Kuril Islands, outside the exclusive economic zones (EEZ) of Japan and Russia. The annual catch of saury by these countries and regions generally increased from the 1990s to the 2000s, with the lowest values in 1998 and 1999 (158–160 thousand tons) and the highest values in 2008 (617 thousand tons) and 2014 (627 thousand tons) (The North Pacific Fisheries Commission, NPFC). Owing to the increasing commercial, bio-economic and ecological values of saury, it has been recognized as a priority species by the

NPFC (www.npfc.int/priority-species).

Oceanographic variation can strongly affect the populations and distribution of saury (Syah et al., 2016; Ueno et al., 2017). Large-scale climatic dynamics have been shown to influence environmental conditions, leading to rapid changes in saury abundance and habitat (Tian et al., 2004). The saury has a lifespan of around two years (Suyama et al., 2006), and its annual catch fluctuated significantly during the last half century (Tian et al., 2002). Previous studies have found that the saury fishing grounds are influenced by oceanographic factors, such as sea surface temperature (SST) (Tseng et al., 2014), and sea surface height (SSH) (Kuroda and Yokouchi, 2017). SST has been demonstrated to perform well when predicting fish habitat (Syah et al., 2016; Yen et al., 2012; Yu et al., 2016), and the preferred SST for saury has been found to vary among life or physiological stages, such as growth, feeding and spawning (Kurita, 2006). For example, saury larvae were found in areas where SST varied from 10.4 to 23.6 °C (Oozeki et al., 2004), and Syah et al. (2017) reported that the favourable habitat of saury was within the SST range 14–16.5 °C. Additionally, SST can affect the onset for saury migration (Kuroda and Yokouchi, 2017). SSH was closely related to vortex flows (Alves et al., 2001), which have a close

* Corresponding author at: College of Marine Sciences, Shanghai Ocean University, Shanghai, 201306, China.

E-mail address: cxhua@shou.edu.cn (C. Hua).



connection to the fishing ground formation of saury (Itoh and Sugimoto, 2002). High probabilities of saury occurrence have been observed in regions where SSH is generally between 0.095 and 0.734 m (Chang et al., 2018). Sea surface temperature gradient (SSTG) was studied for the chub mackerel fishery in the East China Sea (Li et al., 2014) and the coastal saury fishery off Japan (Kimura et al., 2004). A low SSTG was likely to be the preferred oceanographic characteristics for chub mackerel, and their habitats were primarily located on the warmer side of the thermal fronts (Li et al., 2014).

Understanding the spatiotemporal dynamics of fish habitat can support sustainable exploitation and fishery management (Valavanis et al., 2008). Habitat assessment models, such as the generalized additive models (GAMs) (Mugo et al., 2010; Syah et al., 2017), maximum entropy models (MaxEnt) (Alabia et al., 2015; Syah et al., 2016), and habitat suitability index (*HSI*) models (Chen et al., 2010; Tian et al., 2009), can fit the relation between fish distribution and abundance. The *HSI* model has been widely applied to explore the relationship between fishery habitat and oceanographic conditions and to describe habitat suitability due to its superior performance and reliable predictions for certain scenarios (e.g., inadequate geographical sampling and inaccurate assessment of absence data) (Yu et al., 2016). There are various ways to establish an *HSI* model (Fukuda et al., 2011). The associations between the abundance or distribution of fish species and oceanographic variables are often non-linear (Li et al., 2014) because fish schools prefer to aggregate in areas with suitable biotic and abiotic conditions. The yield-density model is a reciprocal quadratic function that has been used to describe the link between the yield of crops and densities of planting (Beaver and Melgar, 1999) and to determine the optimal salinities for copepod species (Xu and Gao, 2011; Xu and Zhang, 2010; Yahuza, 2011).

Generally, all of the oceanographic variables in an *HSI* model are assumed to be weighted equally, but it is obviously unrealistic that all variables have an identical impact on fish distribution (Gong et al., 2012). Boosted regression trees (BRTs) can generate multiple regression trees through random selection and self-learning to improve model stability and prediction accuracy. During computation, a certain amount of data is randomly selected to analyse the effects of independent variables on dependent variables, and the remaining data are used to test the resulting fit. Then, the resulting multiple regression tree is generated as an output as a way to determine the impact load of

Fig. 1. The study area in the Northwestern Pacific Ocean. The blue line represents the Oyashio Current, the black line represents the Kuroshio Extension Current and a warm streamer, and the red circles represent the fishing effort. (For interpretation of the references to colour in this figure legend, the reader is referred to the web version of this article.)

the independent variables on the dependent variables (De'ath, 2007). The relative importance of each independent variable in a BRT analysis can be determined by its contribution to the total variance explained (Xue et al., 2017).

Fishery-independent data have been used to assess fish habitat in many studies (Olivier et al., 2003) but are costly to collect, may lack sufficient spatiotemporal historical coverage (Tian et al., 2009). Although there are known problems with fishery-dependent data, such as the scale of information, sampling bias, and reporting issues (Ochwada-Doyle et al., 2016), studies have increasingly used these data for habitat modelling. In this study, we used fishery-dependent data to develop an *HSI* model. As noted previously, attempts have been made in related studies to illustrate the relationship between oceanographic factors and the distribution of saury using various models, including the *HSI* (Chang et al., 2018; Syah et al., 2016; Tseng et al., 2013). It is important to explore in detail and extend the understanding of the response of saury habitat to monthly oceanographic variability. Furthermore, we aim to analyse the direct mathematical relationship between the suitability index (SI) and oceanographic conditions so that it can be used in the development of high-resolution (e.g., daily) fisheries forecasting systems. Thus saury habitat suitability was established using the yield-density model and weighted statistical analysis. The objectives of this study were: (1) to quantify the dynamic relationship between oceanographic variables and suitable habitat for saury and (2) to explore the spatial distribution of and variation in habitats and potential fishing grounds of saury in relation to oceanographic conditions.

2. Materials and methods

2.1. Data sources and preprocessing

2.1.1. Fishery data

Commercial fishery datasets for the Chinese saury fishery in the Northwestern Pacific Ocean were obtained from the Pacific Saury Technology Group of the China Distant Waters Fisheries Association. These datasets spanned the main fishing seasons of June to November from 2013 to 2016 with a temporal resolution of one day and included: catch (tons), fishing effort (fishing days), longitude and latitude, fishing dates, and ship names. In this study, the catch per unit effort (CPUE) was defined as the daily catch in tonnes per vessel (t/(d·v)). The study

area is shown in Fig. 1.

2.1.2. Oceanographic data

The SST and SSH data from 2013 to 2016 were obtained from remote sensing satellite databases. The daily SST data, which were sourced from the website (<ftp://nordc.noaa.gov>) of the USA's National Oceanic and Atmospheric Administration (NOAA), had a spatial resolution of 0.01° by 0.01° . The daily SSH data were derived from the French Space Agency's Archiving, Validation and Interpolation of Satellite Oceanographic Data (AVISO) at www.aviso.altimetry.fr and had a spatial resolution of 0.25° by 0.25° .

2.1.3. SSTG calculation

Given the depth (15–20 m) at which saury are found (Wada and Kitakata, 1982) and the complex current conditions (e.g., fronts and eddies) in the TZ (Kuroda and Yokouchi, 2017), the horizontal SSTG was included in the analyses. The SSTG was calculated using the gradient magnitude (GM) formula (Pi and Hu, 2010), with the SST value of the current point given as $SST_{i,j}$ (i.e., the value of the SST closest to the fishing location in the grid) and the SSTs of the four adjacent grid points given as $SST_{i+1,j}$, $SST_{i-1,j}$, $SST_{i,j+1}$, and $SST_{i,j-1}$. $SSTG_{i,j}$ (SSTG value of the current point in $^{\circ}\text{C}/\text{km}$) is thus calculated as:

$$SSTG_{i,j} = \sqrt{\left(\frac{SST_{i+1,j} - SST_{i-1,j}}{\Delta x}\right)^2 + \left(\frac{SST_{i,j+1} - SST_{i,j-1}}{\Delta y}\right)^2} \quad (1)$$

where i and j are positive integers that represent the row and column number of the data grid, respectively; Δx represents the longitudinal distance between the $j-1$ column and the $j+1$ column; and Δy represents the latitudinal distance between the $i-1$ row and the $i+1$ row, with both distances in km.

2.1.4. Matching fishery data to oceanographic data

The daily oceanographic grid data closest to the date and location (latitude and longitude) of the daily fishing date were used to most accurately match the oceanographic and fishery data. Monthly oceanographic data were used to create maps of each environmental variable and the predicted *HSI* distribution.

2.2. Data analysis

2.2.1. Suitability index model

Vessels that use stick-held dip nets and fishing lamps tend to concentrate in regions with a high density of saury and they are likely to leave when the catch rate decreases, i.e., an area of high effort implies the presence of a suitable site for saury (Chang et al., 2018). In other words, the distribution of fishing effort is not random; it closely follows the distribution of suitable habitats that support a large saury population, and reflecting the abundance or aggregation of saury. Therefore, the fishing effort was adopted in this study to predict the probability of saury occurrence and was used in combination with variables SST, SSTG, and SSH to establish the SI models. The procedure involved three steps:

- I The SI value in the class interval of each oceanographic variable with the highest effort was set as 1, and the SI was calculated as (Chen et al., 2009):

$$SI_{i(k)} = \frac{Effort_{i(k)}}{Effort_{max}} \quad (2)$$

where $i(k)$ ($k = 1, 2, 3$) represents the class interval of the oceanographic variables (SST, SSTG, and SSH, respectively); $Effort_{i(k)}$ is the fishing effort in class interval $i(k)$; and $Effort_{max}$ refers to the highest fishing effort across all class intervals.

- II Fig. 2 shows there appears to be a normal or log-normal distribution relationship between fishing effort and the variables SST, SSTG, and

SSH, which implied that the oceanographic variables could be better fitted to the fishing effort using a reciprocal quadratic function, as the relationship between the SI and the oceanographic variables could then be established by the yield-density model (Holliday, 1960). In this model, the monthly SI data were fitted to the monthly SST, SSTG, and SSH data to generate a relational model. The equation for the yield-density model is described as (Bleasdale and Nelder, 1960):

$$y = \frac{1}{(a + bx + cx^2)} \quad (3)$$

where y is the SI fitting variable (i.e., $\hat{SI}_{sst,m,i(k)}$, $\hat{SI}_{sstg,m,i(k)}$, and $\hat{SI}_{ssh,m,i(k)}$) for each oceanographic variable (SST, SSTG, and SSH), where $m = 6, 7, \dots, 11$ denote the months of June–November; and x is the mean value of the oceanographic variables within the respective class interval $i(k)$, namely, $SST_{m,i(k)}$, $SSTG_{m,i(k)}$, and $SSH_{m,i(k)}$ for the oceanographic variables SST, SSTG, and SSH, respectively, with a , b , and c as three parameters of the model. Eq. (3) is a hyperbolic function with a maximum value in the first quadrant of the Cartesian coordinate system, thereby making it applicable for inferring the relationship between resource abundance and oceanographic variables and meeting the requirements of this study (Xu, 2008; Xu and Gao, 2011; Xu and Zhang, 2010). Several preconditions are required to use this model, including a large amount of collected fishery data in the study area and a wide range of environmental factor data available. The optimal factors (i.e., SST, SSTG, and SSH) can be calculated if the curve is continuous and has a peak interval (Silverman, 2003), as shown in Fig. 3. Parameters a , b , and c were derived using the Marquardt method based on the estimated SI values and oceanographic variables (Marquardt, 1963), and then the quasi-Newton method for determining non-linear least squares (Yabe and Takahashi, 1991) was employed to estimate the parameters in the model. The measures of goodness of fit of different models were evaluated with corresponding parameters, and the best model was selected by the maximum R^2 . To maximize y , the function y' (4) was derived from Eq. (3), and if $y' = 0$, then $x = -b/2c$, from which the optimal oceanographic values of $-Opt_{sst,m}$, $Opt_{sstg,m}$, and $Opt_{ssh,m}$ —could be calculated accordingly (Christensen, 1996; Xu and Gao, 2011), Eq. (4):

$$y' = \frac{b + 2cx}{(a + bx + cx^2)^2} \quad (4)$$

III To select the appropriate class interval for each oceanographic variable, the SI was fitted with the oceanographic variables in a variety of class intervals within a given interval range chosen specifically for different variables (Table 1), and the optimal class interval $i(k)$ was selected according to the highest R^2 of the fit. After determining the appropriate class interval, bootstrapping (Jean and Anne, 2012) based on 1000 resamples was used to generate distributions for the optimal oceanographic values.

2.2.2. Weight analysis

Weights assigned to different variables based on literature reviews, expert opinions, or identical values could lead to uncertainty and errors. Therefore BRTs based on the “gbm” function in R (Elith and Leathwick, 2008) were used to determine the contribution rate of each variable (SST, SSTG, and SSH) to the *HSI* model. The sampling rate (train.fraction) was 0.8, and the calculation was repeated 1000 times. The weight distributions of SST, SSTG, and SSH in each month, denoted as $\bar{W}_{sst,m}$, $\bar{W}_{sstg,m}$, and $\bar{W}_{ssh,m}$, respectively, were obtained.

2.2.3. HSI modelling

The *HSI* model was used to determine the range of oceanographic variables corresponding to the optimal habitat index, which often produced an approximately bell-shaped curve (Austin, 2007). In this

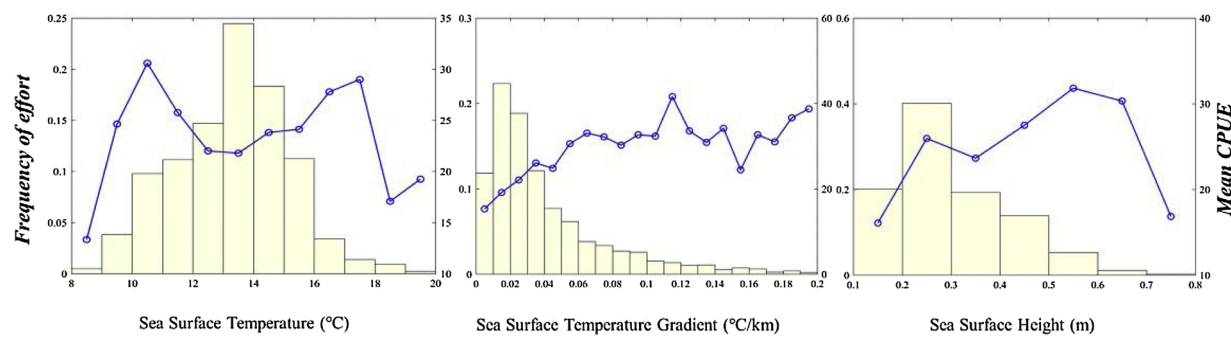


Fig. 2. The frequency of effort and mean CPUE variation with SST, SSTG, and SSH. The histograms represent the frequency of effort, and blue lines represent the mean CPUE. (For interpretation of the references to colour in this figure legend, the reader is referred to the web version of this article.)

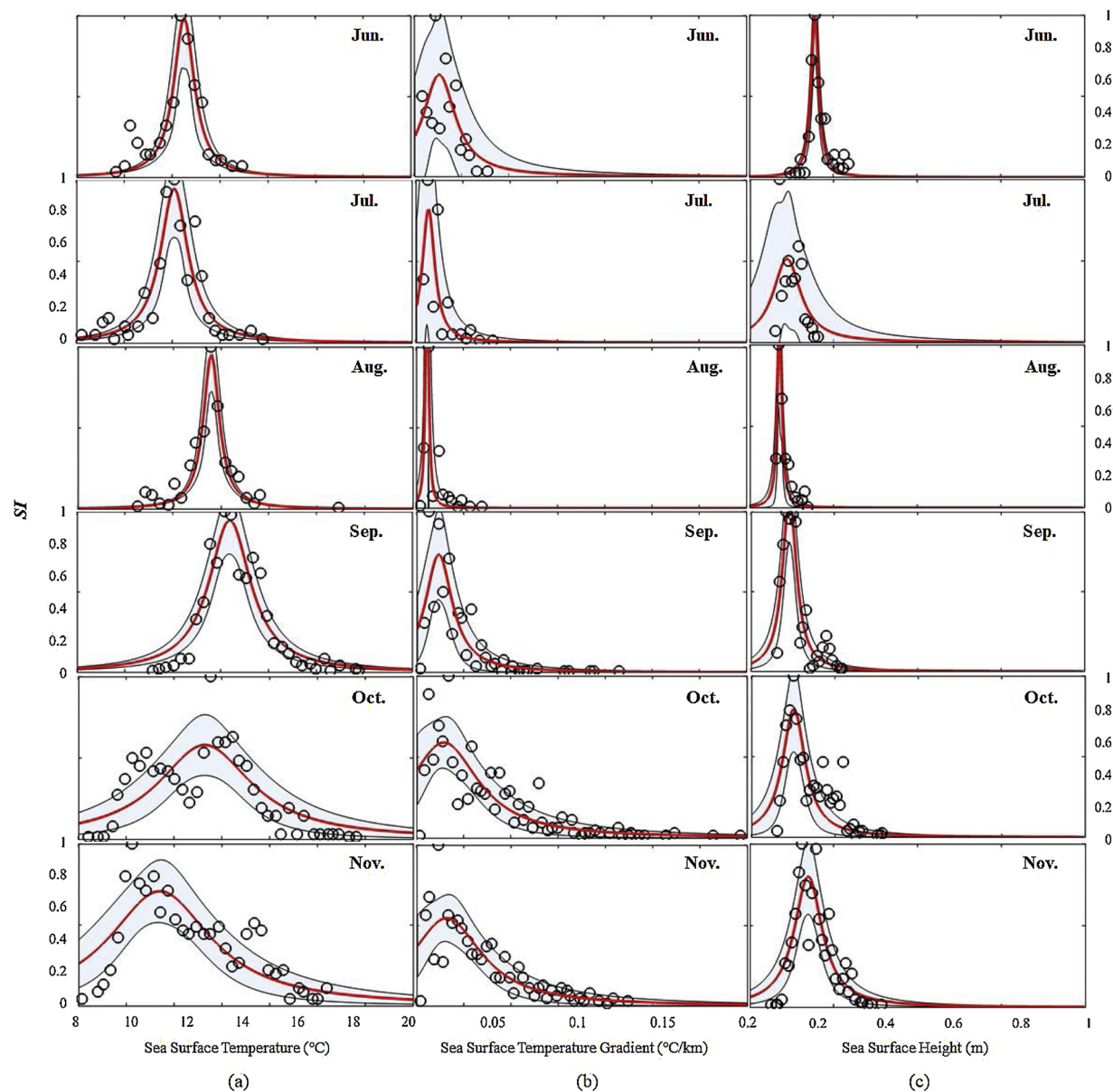


Fig. 3. SI and curve fitting based on SST (a), SSTG (b), and SSH (c) from June to November. Small circles represent the raw observation data used for fitting; red lines represent the yield-density model-fitted curves, and black lines represent 95% confidence intervals of the fitted curves. (For interpretation of the references to colour in this figure legend, the reader is referred to the web version of this article.)

Table 1

Optimal interval values of oceanographic variables.

Oceanographic Variable	Unit	Minimum	Maximum	Interval Range	Interval Step	Reasonable Value*	R^2	Optimal Value
SST	°C	8.07	19.75	0.1-1.0	0.1	0.1	0.5863	0.3
						0.2		
						0.3		
SSTG	°C/km	0	0.34	0.001-0.01	0.001	0.002	0.4276	0.005
						0.003		
						0.004		
						0.005		
SSH	m	0.13	0.84	0.01-0.1	0.01	0.02	0.7563	0.02
						0.03		
						0.04		

The symbol * indicates that SI can be adequately fitted to the oceanographic variables with the class intervals of the oceanographic variables.

study, a weight-based *HSI* model was established based on the arithmetic mean method (Gong et al., 2011) as follows:

$$HSI_m = \hat{SI}_{sst,m} \cdot \bar{W}_{sst,m} + \hat{SI}_{sstg,m} \cdot \bar{W}_{sstg,m} + \hat{SI}_{ssh,m} \cdot \bar{W}_{ssh,m} \quad (5)$$

HSI values between 0 and 1 were assigned to each oceanographic factor, depending on the suitability of the habitat for survival, growth, and reproduction (Vinagre et al., 2006). An *HSI* value of 0 indicated that the conditions were unsuitable for the species, an *HSI* value of 0.5 tended to represent average quality (Vélez-Espino, 2006), and an *HSI* of 1 was assigned to the most favourable habitat. Considering the broad areas where the saury can aggregate during migration, an *HSI* value above 0.5 was then defined as a suitable criterion for saury. Based on the abovementioned weight-based *HSI* model, the monthly spatial distribution of *HSI* in fishing grounds from 2013 to 2015 was calculated and superimposed on the actual fishing sites to examine the feasibility of fishing ground prediction.

2.2.4. Model validation

The *HSI* model was developed using fishery and oceanographic data from 2013 to 2015. The oceanographic data from 2016 were then used to estimate the *HSI*, which was then compared with the fishing effort data in 2016 to validate the model. With the exception of the weight analysis performed using R (R core team, 2017), the statistical analyses and plotting were conducted in MATLAB (2016).

3. Results

3.1. Selection of class intervals for oceanographic variables

The class interval, step size, and SI fitting results for each oceanographic variable are shown in Table 1. The SI could be fitted when the class intervals of SST, SSTG and SSH were within the ranges of 0.1–0.3 °C (step size of 0.1 °C), 0.002–0.005 °C/km (step size of 0.001 °C/km), and 0.02–0.04 m (step size of 0.01 m), respectively. The optimal class intervals were 0.3 °C for SST, 0.005 °C/km for SSTG, and 0.02 m for SSH according to the highest R^2 .

3.2. SI of the oceanographic variables

The SI was fitted to curves based on SST, SSTG, and SSH to generate the monthly functions of $\hat{SI}_{sst,m}$, $\hat{SI}_{sstg,m}$, and $\hat{SI}_{ssh,m}$, respectively. Values of the parameters a , b , and c for the yield-density model are shown in Table 2.

The optimal ranges of the oceanographic variables ($SI > 0.5$) proved to differ among months and tended to vary among fishing seasons (Fig. 3; Table 2). In general, from June to November, the optimal SST range was 8–18 °C, with the mean range of Opt_{sst} extending from 11.41 (SD = 0.35) to 14.38 (SD = 0.39) °C. For SSTG, the optimal range was 0–0.2 °C/km, with the mean range of Opt_{sstg} extending from 0.012 (SD = 0.0013) to 0.032 (SD = 0.0014) °C/km. The optimal range

of SSH was found to be 0.1–0.4 m, with the mean range of Opt_{ssh} extending from 0.18 (SD = 0.07) to 0.4 (SD = 0.13) m.

3.3. Weight calculation

The impact load of each oceanographic variable on SI was calculated from the BRT (Table 3). The weight distribution of the three factors showed that the $\bar{W}_{sst,m}$ ranged from 31.99% to 34.87%, the $\bar{W}_{sstg,m}$ ranged from 34.71% to 43.79%, and the $\bar{W}_{ssh,m}$ ranged from 24.22% to 31.37%. The results indicated that the weight of each variable changed monthly, but the relative impact loads of SST, SSTG, and SSH on SI followed the order of $\bar{W}_{sstg,m} > \bar{W}_{sst,m} > \bar{W}_{ssh,m}$ in all months.

A t-test performed on the monthly weight of oceanographic variables (Table 4) revealed that except for the four weight pairs of $\bar{W}_{sst,6}$ vs. $\bar{W}_{sst,8}$, $\bar{W}_{sst,7}$ vs. $\bar{W}_{sst,10}$, $\bar{W}_{ssh,7}$ vs. $\bar{W}_{ssh,9}$, and $\bar{W}_{ssh,10}$ vs. $\bar{W}_{ssh,11}$, which did not present significant intra-pair differences ($p > 0.05$), there were significant differences between the weights in other months ($p < 0.01$). Thus, the $\bar{W}_{sst,m}$, $\bar{W}_{sstg,m}$, and $\bar{W}_{ssh,m}$ were adopted as the weights of SST, SSTG, and SSH, respectively (Fig. 4), and were used to establish the month-dependent *HSI* model of saury per Eq. (5).

3.4. Validating the *HSI* model

The percentages of fishing effort and CPUE in each stratum of the *HSI* from June to November 2016 were estimated based on the corresponding oceanographic data (Table 5). Approximately 70% of the fishing effort occurred in the high-*HSI* region ($HSI > 0.5$), especially in September. Concurrently, the CPUE values fluctuated for each *HSI* class.

3.5. Spatial distribution of the *HSI*

The *HSI* spatial distribution in the given months from 2013 to 2015 was predicted and compared to the actual fishing effort (Fig. 5), revealing that the fishing vessels were mainly concentrated in areas with high *HSI* values. The monthly *HSI* distribution indicated that the high-*HSI* areas were narrow in extent and shifted from south to north during the months of June to August; however, the high-*HSI* areas appeared to be larger and shifted from north to south during September to November. *HSI* prediction maps among years revealed that the monthly distributions in 2013 and 2014 were similar; however, the *HSI* distributions during July to September in 2015 were located farther southward than those in 2013 and 2014, and the suitable habitats were widely distributed but had low *HSI* values in August 2015. Notably, the distribution of high-*HSI* values in July and August were more complex and disordered than in other months for all years studied. The fishing effort distribution in most months matched the *HSI* maps well, apart from those in July and August 2015. The CPUE showed similar monthly variation in each year (Fig. 6), with the lowest values in June and August and the highest values from September to November, which was consistent with the variations in habitat area size in Fig. 5.

Table 2

Fitted suitability index parameters of saury based on the yield-density model from June to November.

Month	Variable	a	b	c	R ²	$\bar{O}_{pt}(sd)$	95% Confidence Interval of Optimal Value
Jun.	SST	583.34	-93.18	3.73	0.8881	12.50(0.29) °C	[12.45,12.56]
	SSTG	4.18	-195.19	3665.44	0.5351	0.027(0.0019) °C/km	[0.024,0.029]
	SSH	215.12	-1091.63	1319.39	0.9217	0.40(0.13) m	[0.34,0.47]
Jul.	SST	318.29	-52.52	2.17	0.8422	12.08(0.32) °C	[12.02,12.13]
	SSTG	4.87	-531.42	19345.71	0.6041	0.014(0.0013) °C/km	[0.010,0.018]
	SSH	11.30	-84.74	191.88	0.3718	0.22(0.06) m	[0.15,0.32]
Aug.	SST	1209.27	-177.95	6.55	0.9274	13.57(0.36) °C	[13.49,13.65]
	SSTG	23.84	-3965.27	169243.30	0.8650	0.012(0.0013) °C/km	[0.009,0.015]
	SSH	111.06	-1234.85	3460.01	0.9304	0.18(0.07) m	[0.15,0.21]
Sep.	SST	197.69	-27.35	0.95	0.8906	14.38(0.39) °C	[14.32,14.44]
	SSTG	3.89	-213.11	4492.13	0.7183	0.024(0.0015) °C/km	[0.021,0.028]
	SSH	19.99	-165.06	356.97	0.8868	0.23(0.08) m	[0.20,0.25]
Oct.	SST	55.12	-8.04	0.30	0.5966	13.29(0.32) °C	[13.20,13.37]
	SSTG	2.41	-48.93	837.59	0.6734	0.029(0.0017) °C/km	[0.022,0.035]
	SSH	13.22	-93.97	184.50	0.6690	0.25(0.10) m	[0.20,0.32]
Nov.	SST	28.67	-4.78	0.21	0.6252	11.41(0.35) °C	[11.36,11.51]
	SSTG	2.74	-56.65	885.93	0.6803	0.032(0.0014) °C/km	[0.028,0.037]
	SSH	16.06	-84.92	121.72	0.7579	0.35(0.11) m	[0.33,0.37]

Table 3

Monthly weights of the oceanographic variables from June to November.

Variable	Jun.	Jul.	Aug.	Sep.	Oct.	Nov.
$\bar{W}_{sst,m}$	32.09%	33.95%	31.99%	34.87%	33.92%	33.47%
95% CI of $W_{sst,m}$	[31.89%, 32.28%]	[33.71%, 34.19%]	[31.80%, 32.18%]	[34.65%, 35.08%]	[33.76%, 34.09%]	[33.26%, 33.69%]
$\bar{W}_{sstg,m}$	43.04%	38.15%	43.79%	37.05%	34.71%	35.18%
95% CI of $W_{sstg,m}$	[42.83%, 43.24%]	[37.94%, 38.37%]	[43.58%, 43.99%]	[36.82%, 37.29%]	[34.53%, 34.89%]	[34.95%, 35.40%]
$\bar{W}_{ssh,m}$	24.87%	27.90%	24.22%	28.08%	31.37%	31.35%
95% CI of $W_{ssh,m}$	[24.72%, 25.03%]	[27.71%, 28.09%]	[24.06%, 24.39%]	[27.90%, 28.26%]	[31.17%, 31.56%]	[31.17%, 31.53%]

Table 4

t-test of the inter-monthly differences in the oceanographic variables from June to November.

Variable	Jun.	Jul.	Aug.	Sep.	Oct.	Nov.
SST	Jun.		-12.174	0.7216	-18.470	-14.498
	Jul.	0.0000		12.285	-5.4113	0.1460
	Aug.	0.4723*	0.0000		-18.913	-14.684
	Sep.	0.0000	0.0000	0.0000		6.8382
	Oct.	0.0000	0.8842*	0.0000	0.0000	
SSTG	Nov.	0.0000	0.0026	0.0000	0.0000	0.0005
	Jun.		31.6127	-4.9551	38.678	65.873
	Jul.	0.0000		-35.226	7.1668	24.775
	Aug.	0.0000	0.0000		42.618	64.379
	Sep.	0.0000	0.0000	0.0000		15.549
SSH	Oct.	0.0000	0.0000	0.0000	0.0000	
	Nov.	0.0000	0.0000	0.0000	0.0000	0.0009
	Jun.		-24.098	5.8057	-26.766	-52.753
	Jul.	0.0000		28.320	-1.4495	-26.083
	Aug.	0.0000	0.0000		-31.509	-54.970
SSG	Sep.	0.0000	0.1504*	0.0000		-23.749
	Oct.	0.0000	0.0000	0.0000	0.0000	
	Nov.	0.0000	0.0000	0.0000	0.0000	0.1410
						0.8882*

The data above the dotted line are the t values of the oceanographic factor, the data under the line are the corresponding P values, and * ($p > 0.05$) indicates that there is no significant difference between the weights of oceanographic variables in the two months. The values “0.0000” in the above table indicates P values less than 0.0001.

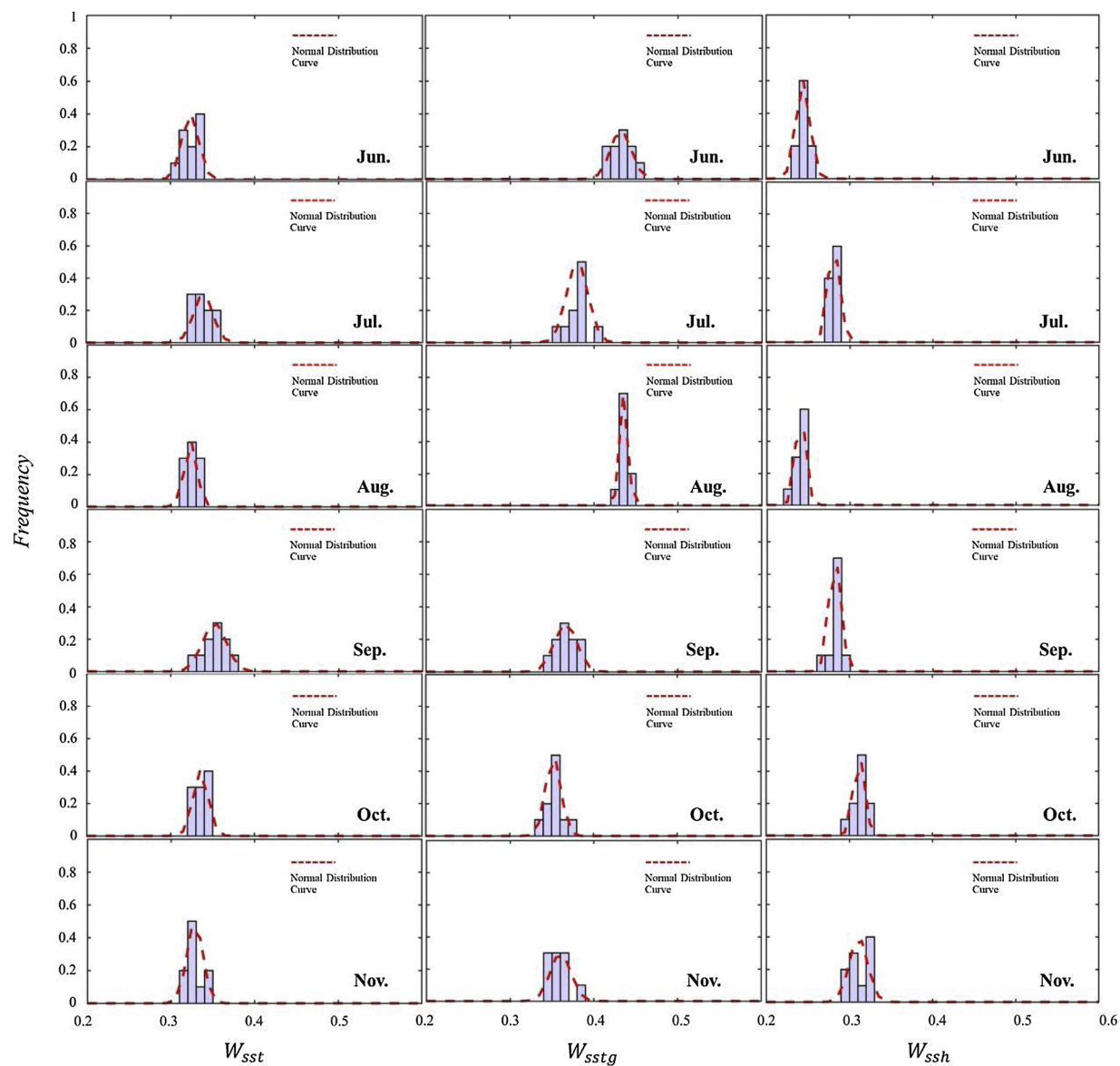


Fig. 4. Weights of oceanographic variables for each month from June to November. The specific *P* values in each cell are listed in Table 4.

Table 5

Percentages of fishing effort and CPUE in each HSI stratum from June to November 2016.

HSI	Jun.		Jul.		Aug.		Sep.		Oct.		Nov.	
	Fishing effort (%)	CPUE										
0.0-0.1	-	-	-	-	2.86	10.00	0.75	10.16	-	-	-	-
0.1-0.2	-	-	1.85	9.50	7.14	8.30	2.99	16.68	7.62	24.69	1.43	22.24
0.2-0.3	4.55	10.36	5.56	10.87	8.57	9.14	4.48	18.64	4.48	23.43	8.57	20.36
0.3-0.4	13.67	11.50	9.26	13.16	5.71	8.99	7.46	16.28	5.38	26.50	8.57	25.12
0.4-0.5	13.64	14.65	13.89	11.91	5.71	11.26	9.70	19.53	16.59	28.81	14.29	27.09
0.5-0.6	18.18	13.48	46.30	14.19	20.00	10.78	23.13	24.98	48.88	34.31	48.57	29.46
0.6-0.7	22.73	16.01	19.44	16.24	22.86	8.71	20.90	23.37	17.04	31.55	18.57	28.01
0.7-0.8	27.27	14.76	3.70	11.42	18.57	10.83	24.63	21.60	-	-	-	-
0.8-0.9	-	-	-	-	5.71	10.66	5.97	20.65	-	-	-	-
0.9-1.0	-	-	-	-	2.86	12.82	-	-	-	-	-	-

The dash “-” in table indicates cases in which fishery data were unavailable.

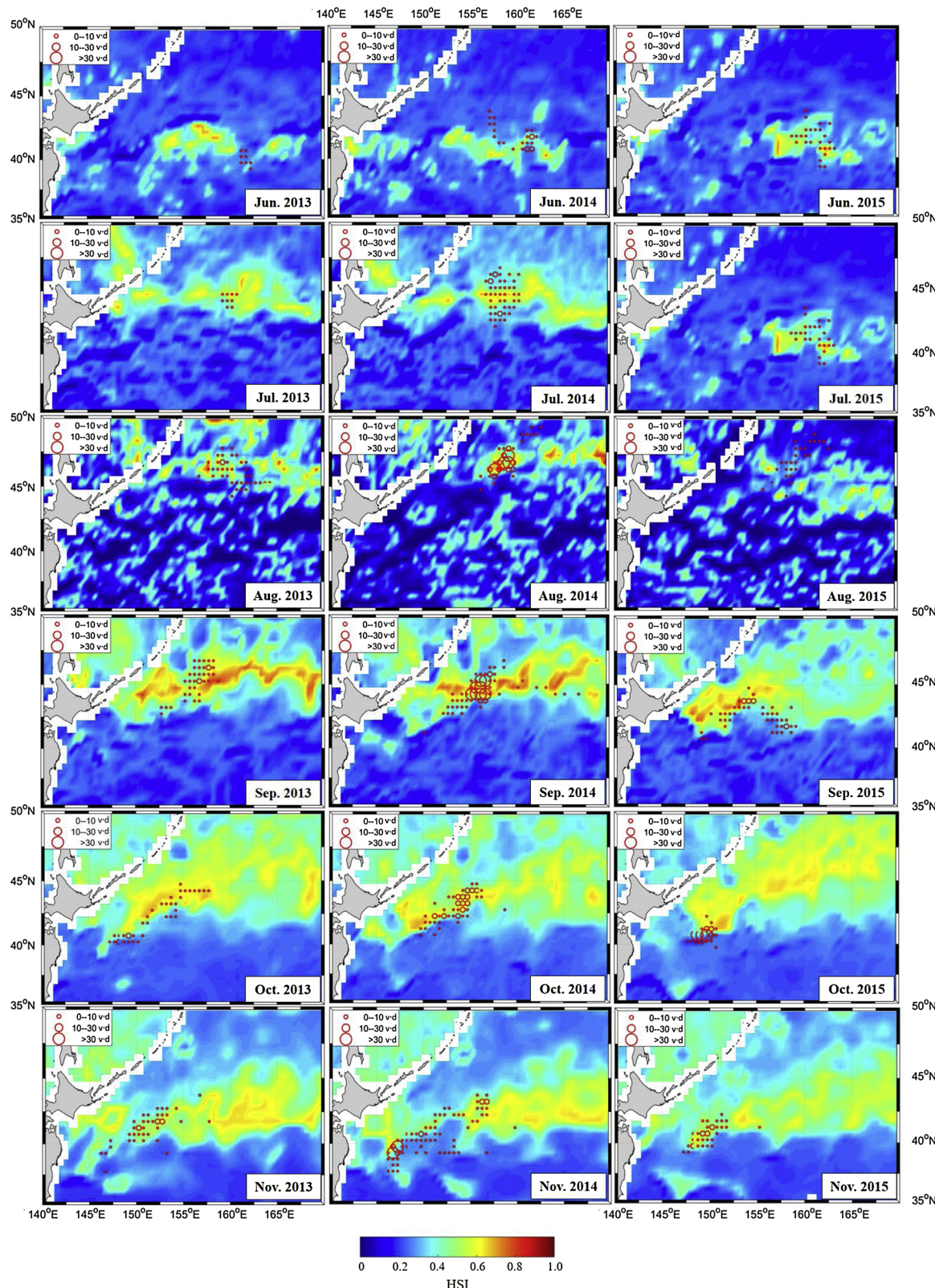


Fig. 5. Distribution of the HSI and fishing effort in the Pacific saury fishing grounds from June to November during 2013–2015.

4. Discussion

4.1. Oceanographic variable selection and the SI model

Oceanographic conditions are known to significantly influence the formation of fishing grounds (Alabia et al., 2015; Kuroda and Yokouchi,

2017). SST and SSH have been frequently applied to predict potential habitats for saury (e.g., Chang et al., 2018; Syah et al., 2017; Tseng et al., 2013). SST has even been considered to be the most important factor affecting the distribution of saury (Syah et al., 2016), while SSH was determined to reveal the mass movement of water and the flow of nutrients, thereby indirectly indicating productivity (Ayers and Lozier,

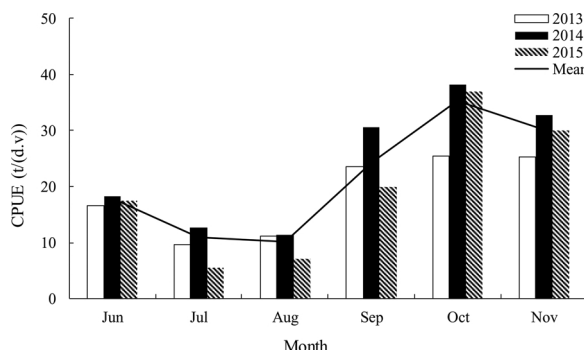


Fig. 6. Monthly CPUE variations of the Chinese Pacific saury from June to November during 2013–2015. The "Mean" in the legend represents the mean CPUE of three years.

2010). Furthermore, to our knowledge, this study is the first to use the horizontal SSTG to investigate saury habitat in the high seas of the North Pacific Ocean. Interestingly, weight analysis indicated that SSTG was the most important impact factor for habitat prediction in each month. To some extent, this may be due to the close relationship between SSTG and eddies and temperature fronts, which are long-term and persistent features in the TZ (Tseng et al., 2014). Convergent oceanographic situations could improve the hydrodynamic conditions and food availability for fish species (Royer et al., 2004). Hence, the analysis of SSTG may be another way to study the effects of temperature fronts and water masses on the distribution of saury. In addition to the above three variables, sea surface salinity (SSS) (Chang et al., 2018) and sea surface Chlorophyll concentration (Chl-a) (Semedi et al., 2002) have been used to describe the relationship between oceanographic conditions and saury distribution. However, daily SSS and Chl-a data with high spatial and temporal resolution were unavailable due to the limitations imposed by cloud interference. More importantly, SSS exhibits a more conservative nature in the high seas (Takasuka et al., 2014), and fishing fleets for saury were found in waters with both low and high Chl-a, reflecting a relatively vague relationship between Chl-a and saury habitat (Semedi et al., 2002). These findings seem to imply that the exclusion of these variables in this study may be appropriate. Therefore, our final selection of SST, SSTG, and SSH is likely suitable for identifying the optimal range for saury habitats throughout the fishing season.

An important part of *HSI* modelling involves fitting and quantifying the relationships between the SI and the oceanographic variables (Li et al., 2014). For each individual oceanographic variable, a high abundance index may correspond to a high SI value, but a high individual SI does not necessarily equate to a high *HSI* value because all other SIs may not be in equilibrium (Tian et al., 2009). Correspondingly, there are uncertain relations among each of the oceanographic factors, and SI modelling methods with better performance could be adopted (Terrell and Carpenter, 1997). The yield-density model has only one peak value in quadrant I that satisfies the possibility of evaluating the favourable oceanographic characteristics for marine organisms (Xu and Zhang, 2010). Based on the results presented in Table 2 and Fig. 3, it could be preliminarily assumed that the relationships between the SI and SST, SSTG, and SSH were reflected by the yield-density model.

4.2. Fishing effort and *HSI* model

The fishing effort data were used to fit the SI curves, as suggested by previous studies (e.g., Chen et al., 2010; Swain and Wade, 1993; Tian et al., 2009). Oceanographic conditions determine the distribution and dynamics of fishery species, influencing the locations of productive fishing grounds and consequently the location of fishing vessels (Postuma and Gasalla, 2010). Therefore, the distribution of fishing

effort is not random; however, the CPUE might be at a low level when both catches and efforts are low or both high, and it might be high with a low catch but with lower efforts (Li et al., 2014). We developed a CPUE-based SI model for each environmental variable, and it seemed that CPUE did not perform better than effort, especially for the SSTG (see Supplementary material S1). Fishing effort was identified as an index capable of detecting suitable saury habitat given that fishing for saury is highly targeted.

Fish habitat is affected by multiple oceanographic variables simultaneously; as such, an *HSI* model combined with the SIs of different variables can be more convenient and can more directly explain the relationship between oceanographic conditions and fisheries than other assessment models, such as GAMs and MaxEnt. The weighting results (Table 3) indicated that the performance of the developed weight-based *HSI* model was better than that of an unweighted *HSI* model. Xue et al. (2017) further reported that a weighted *HSI* model developed by BRT tended to yield a more reliable predictions of suitable habitats for American lobster. Therefore, the mathematical relationship between fisheries and oceanographic conditions derived from this model may be more flexible and accurate in fishery forecasting than traditional approaches using statistical methods.

The outputs of the *HSI* model in Table 5 showed that the majority of the yield during the period of June–November 2016 was obtained in areas with *HSI* > 0.5, providing validation that our model realistically represented this fishery. The CPUE varied monthly and was significantly higher from September–November than from June–August (Fig. 6) and increased with *HSI* for each month while fluctuating when *HSI* > 0.4. Chang et al. (2018) noted that the CPUE values in each *HSI* stratum were irregularly variable for the medium-size saury in the Taiwanese fishery, and similar fluctuations were also found in the squid fishery (Yu et al., 2015). In addition, it seemed that the areas with relatively high effort had lower CPUE (Fig. 2), which could be due to the following reasons: (i) the areas where fish were caught were not necessarily those with high biomass, and the fishing vessels might not operate in all the fishing grounds (Chen et al., 2009); (ii) the appropriate levels of oceanographic variables (SST, SSTG, and SSH) within a certain range supported sources of food for fish; however, the conditions could become unsuitable for habitat once outside that range (Gong, 1984). As shown by the SST in Fig. 2, relatively low and high SSTs were accompanied by low effort because both values exceeded the optimal SST range for saury. Relatedly, fewer vessels were active in the areas with conditions that were unfavourable for the fish. On the other hand, when the optimal SST occurred in fishing grounds, more vessels aggregated in the area. Saury fishing is typically a light-luring fishery; therefore, if a large number of vessels are concentrated in areas with optimal SST levels, the influence of the light intensity from other vessels in close proximity may also lead to a decrease in CPUE. Furthermore, variations in SSTG could lead to changes in the atmospheric pressure, flow, and wind field at the sea surface at a mesoscale to small scale (Hoell and Funk, 2013). Additionally, SSH represents the comprehensive effect of dynamic and thermodynamic processes (Li et al., 2014), which are related to mass water exchange (Itoh and Yasuda, 2009). Both the SSTG and SSH are important non-biological indicators that reflect the complexity and productivity of the oceanographic conditions (Balch et al., 1997; Itoh and Yasuda, 2009). To some extent, the higher the SSTG and SSH were, the higher the potential productivity (and therefore CPUE) was; conversely, both the CPUE and fishing operability were lower under excessively complicated marine conditions.

4.3. Impact of oceanographic variables on the schooling of saury

Previous studies have assigned weights to different variables in *HSI* models according to the enumeration method or expert knowledge, which may be subjective (Vinagre et al., 2006). The BRT method can correlate the responses of predictors using binary splitting and has better fitting ability than some conventional methods (such as

multivariate regression, linear and additive regressions) and can fully apply different patterns of training data (Gao et al., 2016). However, inter-vessel behaviour may lead to a lower daily catch for each vessel, which was also affected by the degree of saury aggregation. The daily catch per vessel may be relatively high when saury aggregations are dense; otherwise, it may be lower. Therefore, the inter-vessel influence was not considered when we used BRT to calculate the weight of each oceanographic variable. The results in Table 3 demonstrated that the weights of the three variables varied monthly, indicating that the given weights differed even in adjacent months, possibly due to differences in life stages of the fish (e.g., for spawning and feeding). This aligns with the finding that suitable oceanographic conditions appear to change with life stage in potential saury habitats and migrations (Chang et al., 2018). Among the three oceanographic variables selected in this study, although the relative weights of the different factors changed monthly, SSTG always had the largest impact on the habitat, as evidenced by its high weight in all months. The impact of SSTG was followed by those of SST and SSH, both of which accounted for approximately 30% of the impact load, indicating that temperature was an important factor for schooling and fishing ground formation of saury. As a machine learning method, BRT can explain the fishing ground distribution simply using training data, but there may be unsatisfactory explanation effects when the selected variables are weakened by pseudo-non-fishing grounds or when some important variables are not considered in the model (Gao et al., 2016). Therefore, it was critical to select the appropriate oceanographic variables when the BRT method is used in *HSI* modelling. We selected the three key and widely used oceanographic variables to describe the habitat of saury, which could support the BRT weights. In conclusion, the impact loads of the oceanographic conditions on fishing grounds calculated by the BRT method, rather than the use of subjectively assigned weights for *HSI* modelling, can more accurately reflect the habitat index of fish species.

The main current within the studied region (140–170 °E, 38–48 °N), the Oyashio Current, is strongest in the spring (Ohshima et al., 2005) and gradually weakens from June to August. This leads to a relatively lower number of fronts in the fishing regions and a narrower fishing ground distribution with lower CPUE (Tseng et al., 2014). Additionally, the SSTG may play a larger role in the habitat of saury than other variables during this period, which is validated by the weights shown in Table 3. In addition, due to the increasing weight of SSH from September to November, we can confirm the increase in importance of SSH in affecting the schooling of saury. According to the monthly optimal values of oceanographic variables (Table 2), there were higher SSTG and SSH from September to November in the studied area, especially in October and November. In other words, more complex oceanographic conditions may be associated with a relatively high number of eddies in saury habitats from September to November. In addition, these eddies may trap the prey of saury, creating good feeding conditions by enhancing plankton availability.

We have established that the preferred oceanographic characteristics for saury tend to vary over time. To better understand the monthly spatial variation in oceanographic conditions, superposition maps of SST, SSTG, and SSH from June to November during 2013 to 2015 are shown in Fig. 7. During June to August, the water temperature in the North Pacific Ocean gradually increased and the saury migrated northward, whereas from September to November, the water temperature gradually decreased, and the saury migrated southward. Oceanographic structures, such as the warm-core rings in the Kuroshio Current and the transport path of cold waters associated with the Oyashio intrusions, have been reported to affect the routes, pattern and timing of saury migrations (Itoh and Sugimoto, 2002; Kuroda and Yokouchi, 2017; Watanabe et al., 2006). Additionally, the optimal SST for the early life and spawning periods tended to differ those for other life stages (Takasuka et al., 2016). These findings may demonstrate that SST is an important factor for the changes in migration and aggregation of saury. There have been prior efforts to report the habitat preferences

of the saury; for instance, previous studies have stated that saury fishing grounds mainly exist in areas with SST ranges from 10 to 20 °C (Huang, 2010) and that the optimal range of SSTG in coastal water was 0.8 to 2 °C/km (Kimura et al., 2004). The calculated optimal SST and SSH ranges of the fishing zones for each month, as well as the trend in monthly variation noted in our study, were comparable to those in the previous works. However, there is disagreement regarding the optimal SSTG range, which might be due to the following reasons: (i) Kimura et al. (2004) obtained oceanographic data (including SST) from satellite images and matched the corresponding catch data, meaning that different methods were used to obtain and process the data; (ii) Itoh and Sugimoto (2002) indicated that relatively few fronts were detected in the offshore waters of Japan, but more fronts were found in the coastal waters. Fig. 7 also shows that the oceanographic conditions in the coastal waters were relatively more complex than those in offshore waters. In particular, the low SSTG values found in our work may also be related to differences in the study regions and the numbers of fronts.

4.4. Distribution of and variation in the *HSI*

An accurate prediction of suitable habitats and variations in habitat are essential to support productive fishing. We have depicted the monthly *HSI* distribution maps from 2013 to 2015, and similarly, the general distribution of and variation in *HSI* trends observed in our work are comparable to the results of Syah et al. (2016). The *HSI* maps reveal clear monthly variation, especially the significant reduction in suitable habitat in June and August. Furthermore, the broadly distributed but low *HSI* observed in August illustrates that the optimal habitat for saury was not concentrated during this time and corresponded to the lowest CPUE, as shown in Fig. 6. However, this phenomenon was not identified by Syah et al. (2016) and could be interpreted on the basis of the inter-month SST shown in Fig. 7. The annual variation in SST indicates that the strongest Kuroshio Current principally occurred in August (Ito et al., 2007), with minimum Oyashio transport (Kuroda and Yokouchi, 2017). Additionally, fewer SST fronts were detected in June and August, while more fronts appeared to form in September (Tseng et al., 2014). Furthermore, the weight of SSH was lowest in August (Table 3), which coincided exactly with the irregular *HSI* map. It was estimated that the suitable habitat was formed by a co-influence of several oceanographic variations, which may illustrate the potential mechanism of the comprehensive interaction of oceanographic conditions on the habitat distribution of saury.

As shown in Fig. 5, the interannual *HSI* maps indicated a slightly more southward distribution of *HSI* in 2015 than in 2013 and 2014. This pattern was especially clear during July to September, but not in October and November. Moreover, areas of high-*HSI* in 2013 and 2014 showed a slight expanding trend compared to 2015. Studies have reported that a strong El Niño event occurred in November and December in 2014 and throughout 2015 (Tian et al., 2004), which could have led to higher water temperatures, fewer eddies, and reduced Oyashio transport than during normal years in the North Pacific (Sugimoto et al., 2001). The non-obvious southward movement of the *HSI* during October and November may be caused by the broader and slightly lower *HSI* distribution. On the other hand, the Pacific Decadal Oscillation (PDO) has been positive since 2014 (Trenberth and Fasullo, 2014), enhancing the Oyashio transport off the Hokkaido coast given the atmospheric conditions. This may be another factor leading to the southward movement of the fishing grounds in 2015 and may have had a negative effect on saury abundance (Kuroda and Yokouchi, 2017), in keeping with the higher total catch of saury harvested by all fishing countries and regions in 2013 (422 thousand tons) and 2014 (627 thousand tons) and the lowest catch in 2015 (354 thousand tons) (Chang et al., 2018). In addition, the monthly distribution of high-*HSI* in areas within the EEZ of Japan and Russia was slightly different from that described by Japanese vessels in a previous report (NPFC, 2018). This discrepancy may be because monthly mean oceanographic data

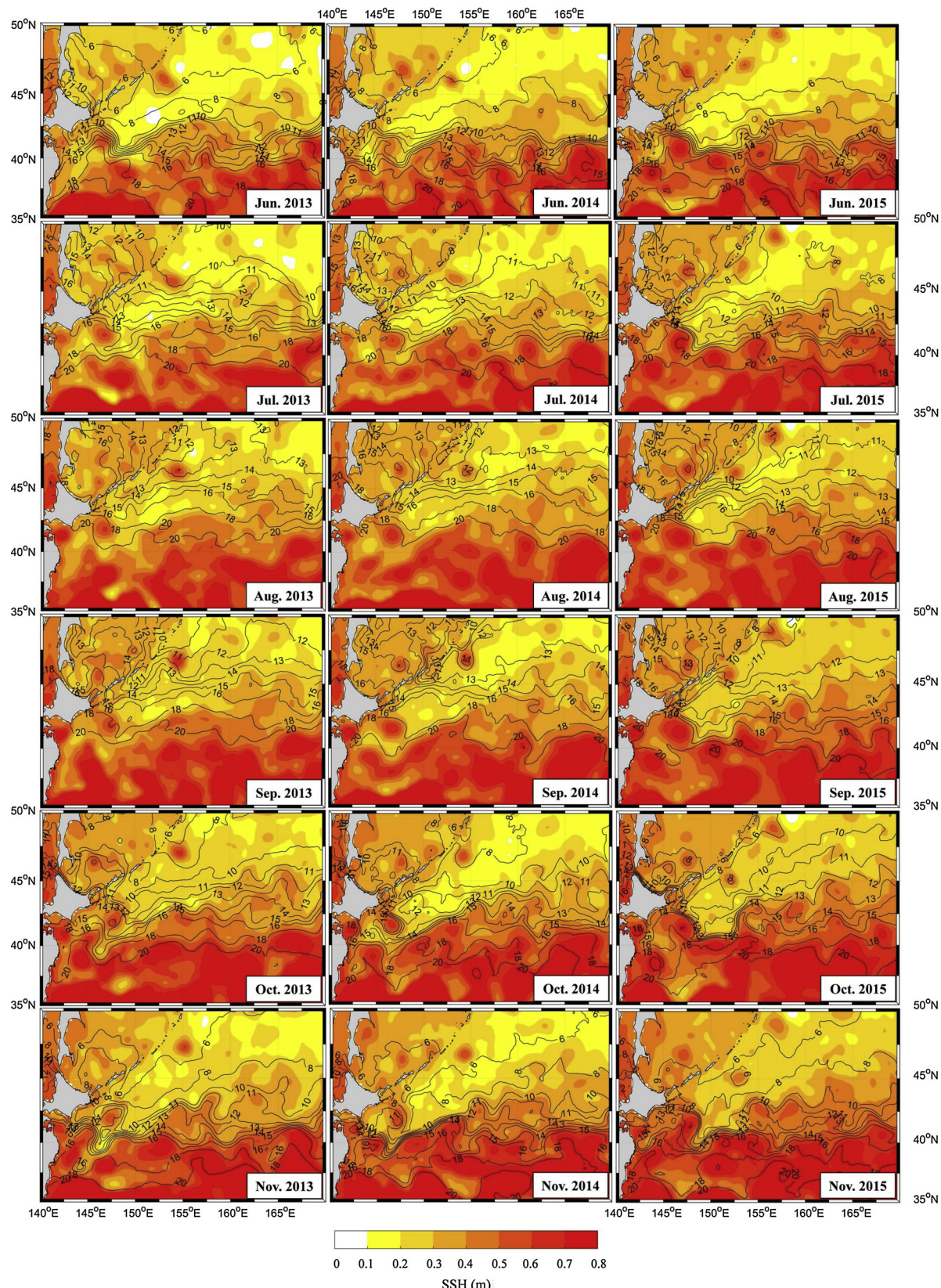


Fig. 7. Monthly superposition maps of SST and SSTG on the SSH from June to November during 2013–2015. The coloured maps represent SSH, the black isotherms represent SST, and the density of isotherms reflects SSTG.

were used to describe the *HSI* distribution in this study, which led to a deviation of the predicted results.

4.5. *HSI* model improvement

We combined the yield-density model and BRT-based weight analysis to quantify the potential suitability of habitat for saury. In view of the complex oceanographic conditions in the Northwestern Pacific Ocean, we recommended that the *HSI* model be used to explore the oceanographic-habitat interactions and to predict spatial variation in saury fishing grounds. Our study achieved a relatively comprehensive understanding of the habitat conditions of saury using three key oceanographic variables; however, there were some drawbacks in the developed *HSI* model. For example, the *HSI* distribution in this study was calculated by mean monthly oceanographic data, which may hamper the *HSI* modelling efforts and increase uncertainty in habitat prediction due to the lower spatiotemporal data resolution. Therefore, further work to integrate additional real-time oceanographic data is required to perform a dynamic analysis of the saury fishing grounds. Furthermore, given the long migration route of saury, additional oceanographic indicators, such as sea surface height anomaly (SSHA), eddy kinetic energy (EKE) (Syah et al., 2016), and Kuroshio warm-core ring (Saitoh et al., 1986), could be incorporated into the *HSI* model to improve the comprehension of the relationships between oceanographic variables and the distribution of saury.

Funding

This study was supported by the Ministry of Science and Technology of China (grant number 2013BAD13B05).

Data availability

The datasets created during and/or analysed in the current study are available from the corresponding author upon reasonable request.

Human and animal rights

All applicable international, national, and/or institutional guidelines for the care and use of animals were followed.

Declaration of Competing Interest

The authors declare that they have no conflict of interest.

Acknowledgements

We thank two anonymous reviewers and editor, Prof. Andre Punt, for their constructive comments and suggestions to improve the quality of the study.

Appendix A. Supplementary data

Supplementary material related to this article can be found, in the online version, at doi:<https://doi.org/10.1016/j.fishres.2019.105408>.

References

- Alabia, I.D., Saitoh, S., Mugo, R., Igarashi, H., Ishikawa, Y., 2015. Seasonal potential fishing ground prediction of neon flying squid (*Ommastrephes bartramii*) in the western and central North Pacific. Fish. Oceanogr. 24, 190–203. <https://doi.org/10.1111/fog.12102>.
- Alves, J.O.S., Haines, K., Anderson, D.L.T., 2001. Sea level assimilation experiments in the Tropical Pacific. J. Phys. Oceanogr. 31 (2), 305–323. [https://doi.org/10.1175/1520-0485\(2001\)031<305:SLAET>2.0.CO;2](https://doi.org/10.1175/1520-0485(2001)031<305:SLAET>2.0.CO;2).
- Austin, M., 2007. Species distribution models and ecological theory: a critical assessment and some possible new approaches. Ecol. Model. 200, 1–19. <https://doi.org/10.1016/j.ecolmodel.2006.07.005>.
- Ayers, J.M., Lozier, M.S., 2010. Physical controls on the seasonal migration of the North Pacific transition zone chlorophyll front. J. Geophys. Res. 115 (C05001), 1–11. <https://doi.org/10.1029/2009JC005596>.
- Balch, W.M., Bowler, B.C., Byrne, C.F., 1997. Sea surface temperature gradients, baroclinicity, and vegetation gradients in the sea. J. Plankton Res. 19 (12), 1829–1858. <https://doi.org/10.1093/plankt/19.12.1829>.
- Beaver, R.J., Melgar, M., 1999. Analysis of yield-density models for intercropping experiments. Biom. J. 41, 995–1011. [https://doi.org/10.1002/\(SICI\)1521-4036\(199912\)41:8<995::AID-BIMJ995>3.0.CO;2-H](https://doi.org/10.1002/(SICI)1521-4036(199912)41:8<995::AID-BIMJ995>3.0.CO;2-H).
- Bleasdale, J.K.A., Nelder, J.A., 1960. Plant population and crop yield. Nature 188 <https://doi.org/10.1038/188342a0>. 342–342.
- Chang, Y.J., Lan, K.W., Walsh, W.A., Hsu, J., 2018. Modelling the impacts of oceanographic variation on habitat suitability for Pacific saury in the Northwestern Pacific Ocean. Fish. Oceanogr. 00, 1–14. <https://doi.org/10.1111/fog.12408>.
- Chen, X.J., Li, G., Feng, B., Tian, S.Q., 2009. Habitat suitability index of Chub mackerel (*Scomber japonicus*) from July to September in the East China Sea. J. Oceanogr. 65, 93–102. http://gdhs.ijournal.cn/hyhzh/ch/reader/create_pdf.aspx?file_no=20090606&year_id=2009&quarter_id=6&falg=1.
- Chen, X.J., Tian, S.Q., Chen, Y., Liu, B.L., 2010. A modeling approach to identify optimal habitat and suitable fishing grounds for neon flying squid (*Ommastrephes bartramii*) in the Northwest Pacific Ocean. Fish. Bull.- Natl. Ocean. Atmos. Adm. 108, 1–14. <https://fisherybulletin.nmfs.noaa.gov/sites/default/files/pdf-content/2010/1081/chen.pdf>.
- Christensen, R., 1996. *Analysis of Variance, Design, and Regression: Applied Statistical Methods*. Chapman and Hall/CRC, Boca Raton, pp. 27–58.
- De'ath, G., 2007. Boosted trees for ecological modeling and prediction. Ecology 88, 243–251. [https://doi.org/10.1890/0012-9658\(2007\)88\[243:BTFEMA\]2.0.CO;2](https://doi.org/10.1890/0012-9658(2007)88[243:BTFEMA]2.0.CO;2).
- Elith, J., Leathwick, J., 2008. A working guide to boosted regression trees. J. Anim. Ecol. 77, 802–813. <https://doi.org/10.1111/j.1365-2656.2008.01390.x>.
- Fukuda, S., Masuda, S., Hiramatsu, K., Harada, M., 2011. Assessing the effects of data types and categorization methods on HSI-based habitat suitability analysis for Japanese Medaka (*Oryzias latipes*). J. Agric. Eng. Soc. Jpn. 79, 55–63.
- Fukushima, S., 1979. Synoptic analysis of migration and fishing conditions of saury in the northwest Pacific Ocean. Bull. Tohoku Reg. Fish. Res. Lab. 41, 1–70 (in Japanese with English abstract).
- Gao, F., Chen, X.J., Guan, W.J., Gang, L.I., 2016. A new model to forecast fishing ground of *Scomber japonicus* in the Yellow Sea and East China Sea. Acta Oceanol. Sin. 35 (4), 74–81. <https://doi.org/10.1007/s13131-015-0767-8>.
- Gong, C.X., Chen, X.J., Gao, F., Chen, Y., 2012. Importance of weighting for multi-variable habitat suitability index model: a case study of winter-spring cohort of *Ommastrephes bartramii* in the Northwestern Pacific Ocean. J. Ocean Univ. China 11, 241–248. <https://doi.org/10.1007/s11802-012-1898-6>.
- Gong, C.X., Chen, X.J., Gao, F., Guan, W.J., Lei, L., 2011. Review on habitat suitability index in fishery science. J. Ocean Univ. Shanghai 20, 260–269. <https://doi.org/10.3724/SP.J.1011.2011.00415>. (in Chinese with English abstract).
- Gong, Y., 1984. Distribution and movement of Pacific saury, *Cololabis saira* (Brevoort) in relation to oceanographic conditions in waters off Korea. Bull. Fish. Res. 33, 59–172. <https://ci.nii.ac.jp/naid/500000018255/>.
- Hoell, A., Funk, C., 2013. The ENSO-related West Pacific sea surface temperature gradient. J. Clim. 26 (23), 9545–9562. <https://doi.org/10.1175/JCLI-D-12-00344.1>.
- Holliday, R., 1960. Plant population and crop yield: part I. Field crop. Nature 13, 159–167. <https://doi.org/10.1038/186022b0>.
- Huang, W.B., 2010. Comparisons of monthly and geographical variations in abundance and size composition of Pacific saury between the high-seas and coastal fishing grounds in the northwestern Pacific. Fish. Sci. 76 (1), 21–31. <https://doi.org/10.1007/s12562-009-0196-8>.
- Ito, S.I., Megrey, B.A., Kishi, M.J., Mukai, D., Kurita, Y., Ueno, Y., Yamanaka, Y., 2007. On the interannual variability of the growth of Pacific saury (*Cololabis saira*): a simple 3-box model using NEMURU. Fish. Ecol. Model. 202 (1), 174–183. <https://doi.org/10.1016/j.ecolmodel.2006.07.046>.
- Itoh, S., Sugimoto, T., 2002. Behavior of warm-core rings in a double-gyre wind-driven ocean circulation model. J. Oceanogr. 58 (5), 651–660. <https://doi.org/10.1023/A:1022838205678>.
- Itoh, S., Yasuda, I., 2009. Characteristics of mesoscale eddies in the Kuroshio-Oyashio Extension region detected from the distribution of the sea surface height anomaly. J. Phys. Oceanogr. 40 (5). <https://doi.org/10.1175/2009jpo4265.1>. 1081–1034.
- Jean, F., Anne, S., 2012. Bootstrap variance estimation with survey data when estimating model parameters. Comput. Stat. Data Anal. 56, 4450–4461. <https://doi.org/10.1016/j.csda.2012.03.011>.
- Kimura, N., Okada, Y., Mahapatra, K., 2004. Relationships between the saury fishing ground and sea surface oceanographic features determined from satellite data along the northeastern coast of Japan. J. Sch. Mar. Sci. Technol. 2 (2), 1–12 (in Japanese with English abstract).
- Kurita, Y., 2006. Regional and interannual variations in spawning activity of Pacific saury *Cololabis saira* during northward migration in spring in the north-western Pacific. J. Fish Biol. 69, 846–859. <https://doi.org/10.1111/j.1095-8649.2006.01159.x>.
- Kuroda, H., Yokouchi, K., 2017. Interdecadal decrease in potential fishing areas for Pacific saury off the southeastern coast of Hokkaido, Japan. Fish. Oceanogr. 26 (4), 439–454. <https://doi.org/10.1111/fog.12207>.
- Li, G., Chen, X.J., Lei, L., Guan, W.J., 2014. Distribution of hotspots of chub mackerel based on remote-sensing data in coastal waters of China. Int. J. Remote Sens. 35 (11–12), 4399–4421. <https://doi.org/10.1080/01431161.2014.916057>.
- Marquardt, M.D., 1963. An algorithm for least-squares estimation of nonlinear parameters. J. Soc. Ind. Appl. Math. 11, 431–441. <https://doi.org/10.1137/0111030>.
- Matsumiya, Y., Tanaka, S., 1976. Dynamics of the saury population in the Pacific Ocean

- off northern Japan, I: abundance index in number by size category and fishing ground. *Nippon Suisan Gakkai Shi* 42, 277–286. <https://doi.org/10.2331/suisan.42.277>.
- Mugo, R., Saitoh, S., Nihira, A., Kuroyama, T., 2010. Habitat characteristics of skipjack tuna (*Katsuwonus pelamis*) in the western North Pacific: a remote sensing perspective. *Fish. Oceanogr.* 19, 382–396. <https://doi.org/10.1111/j.1365-2419.2010.00552.x>.
- NPFC, 2018. North Pacific Fisheries Commission Yearbook 2017. pp. 385. <http://www.npfc.int>.
- Ochwada-Doyle, F.A., Johnson, D.D., Lowry, M., 2016. Comparing the utility of fishery-independent and fishery-dependent methods in assessing the relative abundance of estuarine fish species in partial protection areas. *Fish. Manag. Ecol.* 23 (5), 390–406. <https://doi.org/10.1111/fme.12182>.
- Ohshima, K.I., Wakatsuchi, M., Saitoh, S.I., 2005. Velocity field of the Oyashio region observed with satellite-tracked surface drifters during 1999–2000. *J. Oceanogr.* 61 (5), 845–855. <https://doi.org/10.1007/s10872-006-0004-3>.
- Olivier, P.L., Florence, C., Stéphanie, M., Pascal, L., Daniel, G., Yves, D., 2003. Quantitative description of habitat suitability for the juvenile common sole (*Solea solea*, L.) in the Bay of Biscay (France) and the contribution of different habitats to the adult population. *J. Sea Res.* 50 (2), 139–149. [https://doi.org/10.1016/s1385-1101\(03\)00059-5](https://doi.org/10.1016/s1385-1101(03)00059-5).
- Oozeki, Y., Watanabe, Y., Kitagawa, D., 2004. Environmental factors affecting larval growth of Pacific saury *Cololabis saira* in the Northwestern Pacific Ocean. *Fish. Oceanogr.* 13 (Suppl. 1), 44–53. <https://doi.org/10.1111/j.1365-2419.2004.00317.x>.
- Pi, Q.L., Hu, J.Y., 2010. Analysis of sea surface temperature fronts in the Taiwan Strait and its adjacent area using an advanced edge detection method. *Sci. China Earth Sci.* 53, 1008–1016. <https://doi.org/10.1007/s11430-010-3060-x>.
- Postuma, F.A., Gasalla, M.A., 2010. On the relationship between squid and the environment: artisanal jigging for *Loligo plei* at São Sebastião Island (24°S), southeastern Brazil. *ICES J. Mar. Sci.* 67 (5), 1353–1362. <https://doi.org/10.1093/icesjms/fsq105>.
- R core team, 2017. R: A Language and Environment for Statistical Computing. URL R Foundation for Statistical Computing, Vienna, Austria. <http://www.R-project.org/>.
- Royer, F., Fromentin, J.M., Gaspar, P., 2004. The association between bluefin tuna schools and oceanic features in the Western Mediterranean Sea. *Mar. Ecol.-Prog. Ser.* 269, 249–263.
- Saitoh, S.I., Kosaka, S., Iisaka, J., 1986. Satellite infrared observations of Kuroshio warm-core rings and their application to study of Pacific saury migration. *Deep Sea Res. A Oceanogr.* 33 (11), 1601–1615. [https://doi.org/10.1016/0198-0149\(86\)90069-5](https://doi.org/10.1016/0198-0149(86)90069-5).
- Semedi, B., Saitoh, S., Saitoh, K., Yoneta, K., 2002. Application of multi-sensor satellite remote sensing for determining distribution and movement of Pacific saury, *Cololabis saira*. *Fish. Sci.* 68, 1781–1784.
- Silverman, R.A., 2003. Modern Calculus and Analytic Geometry. Courier Dover Publications, New York.
- Sugimoto, T., Kimura, S., Tadokoro, K., 2001. Impact of El Niño events and climate regime shift on living resources in the western North Pacific. *Prog. Oceanogr.* 49 (1), 113–127. [https://doi.org/10.1016/S0079-6611\(01\)00018-0](https://doi.org/10.1016/S0079-6611(01)00018-0).
- Suyama, S., Kurita, Y., Ueno, Y., 2006. Age structure of Pacific saury *Cololabis saira* based on observations of the hyaline zones in the otolith and length frequency distributions. *Fish. Sci.* 72 (4), 742–749. <https://doi.org/10.1111/j.1442-2906.2006.01213.x>.
- Swain, D.P., Wade, E.J., 1993. Density-dependent geographic distribution of Atlantic cod (*Gadus morhua*) in the southern Gulf of St. Lawrence. *Can. J. Fish. Aquat. Sci.* 50 (4), 725–733. <https://doi.org/10.1139/f93-083>.
- Syah, A.F., Saitoh, S.I., Alabia, I.D., Hirawake, T., 2016. Predicting potential fishing zones for Pacific saury (*Cololabis saira*) with maximum entropy models and remotely sensed data. *Fish. Bull.- Natl. Ocean. Atmos. Adm.* 114, 330–342. <https://doi.org/10.7755/fb.114.330>.
- Syah, A.F., Saitoh, S.I., Alabia, I.D., Hirawake, T., 2017. Detection of potential fishing zone for Pacific saury (*Cololabis saira*) using generalized additive model and remotely sensed data. *IOP Conf. Ser.: Earth Environ. Sci.* 54 (12–18). <https://doi.org/10.1088/1755-1315/54/1/012074>.
- Takasuka, A., Kuroda, H., Okunishi, T., Shimizu, Y., Hirota, Y., Kubota, H., Sakaj, H., Kimura, R., Ito, S.I., Oozeki, Y., 2014. Occurrence and density of Pacific saury *Cololabis saira* larvae and juveniles in relation to environmental factors during the winter spawning season in the Kuroshio Current system. *Fish. Oceanogr.* 23 (4), 304–321. <https://doi.org/10.1002/foag.8059>.
- Takasuka, A., Nishikawa, K., Kuroda, H., Okunishit, A., Shimizu, Y., Sakaj, H., Ito, S.I., Tokai, T., Oozeki, Y., 2016. Growth variability of Pacific saury *Cololabis saira* larvae under contrasting environments across the Kuroshio axis: survival potential of minority versus majority. *Fish. Oceanogr.* 25 (4), 390–406. <https://doi.org/10.1111/fog.12160>.
- Terrell, J.W., Carpenter, J.C., 1997. Selected Habitat Suitability Index Model Evaluations. Information and Technology Report 1997-0005. U.S. Fish and Wildlife Service, pp. 5.
- Tian, S.Q., Chen, X.J., Chen, Y., Xu, L., Dai, X.J., 2009. Evaluating habitat suitability indices derived from CPUE and fishing effort data for *Ommatophterus bratramii* in the northwestern Pacific Ocean. *Fish. Res.* 95, 181–188. <https://doi.org/10.1016/j.fishres.2008.08.012>.
- Tian, Y.J., Ueno, Y., Suda, M., Akamine, T., 2002. Climate-ocean variability and the response of Pacific saury (*Cololabis saira*) in the northwestern Pacific during the last half century. *Fish. Sci.* 68, 158–161. https://doi.org/10.2331/fishsci.68.sup1_158.
- Tian, Y.J., Ueno, Y., Suda, M., Akamine, T., 2004. Decadal variability in the abundance of Pacific saury and its response to climatic/oceanic regime shifts in the northwestern subtropical Pacific during the last half century. *J. Mar. Syst.* 52, 235–257. <https://doi.org/10.1016/j.jmarsys.2004.04.004>.
- Trenberth, K.E., Fasullo, J.T., 2014. An apparent hiatus in global warming? *Earth's Future* 1 (1), 19–32. <https://doi.org/10.1002/2013ef000165>.
- Tseng, C.T., Su, N.J., Sun, C.L., Punt, A.E., Yeh, S.Z., Liu, D.C., Su, W.C., 2013. Spatial and temporal variability of the Pacific saury (*Cololabis saira*) distribution in the northwestern Pacific Ocean. *ICES J. Mar. Sci.* 70 (5), 991–999. <https://doi.org/10.1093/icesjms/fs205>.
- Tseng, C.T., Sun, C.L., Belkin, I.M., Yeh, S.Z., Kuo, C.L., Liu, D.C., 2014. Sea surface temperature fronts affect distribution of Pacific saury (*Cololabis saira*) in the Northwestern Pacific Ocean. *Deep-Sea Res. Part II Top. Stud. Oceanogr.* 107, 15–21. <https://doi.org/10.1016/j.dsr2.2014.06.001>.
- Ueno, Y., Suyama, S., Nakagami, M., Naya, M., Sakai, M., Kurita, Y., 2017. Direct estimation of stock abundance of Pacific saury *Cololabis saira* in the Northwestern Pacific Ocean using a mid-water trawl. *Fish. Sci.* 83 (1), 23–33. <https://doi.org/10.1007/s12562-016-1044-2>.
- Valavanis, V.D., Pierce, G.J., Zuur, A.F., Palialexis, A., Saveliev, A., 2008. Modelling of essential fish habitat based on remote sensing, spatial analysis and GIS. *Hydrobiologia* 612, 5–20. <https://doi.org/10.1007/s10750-008-9493-y>.
- Vélez-Espino, L.A., 2006. Distribution and habitat suitability index model for the Andean catfish *Astroblepus ubidai* (Pisces: Siluriformes) in Ecuador. *Rev. Biol. Trop.* 54, 623–638. <https://doi.org/10.15517/rbt.v54i2.13937>.
- Vinagre, C., Fonseca, V., Cabral, H., Costa, M.J., 2006. Habitat suitability index models for the juvenile soles, *Solea solea* and *Solea senegalensis*, in the Tagus estuary: defining variables for species management. *Fish. Res.* 82 (1), 140–149. <https://doi.org/10.1016/j.fishres.2006.07.011>.
- Wada, T., Kitakata, M., 1982. Sampling research with midwater drift gillnet and behavior of saury in the daytime. *Bull. Hokkaido Reg. Fish. Lab.* 47, 11–22 (in Japanese with English abstract).
- Watanabe, K., Tanaka, E., Yamada, S., Kitakado, T., 2006. Spatial and temporal migration modeling for stock of Pacific saury *Cololabis saira* (Brevoort), incorporating effect of sea surface temperature. *Fish. Sci.* 72 (6), 1153–1165. <https://doi.org/10.1111/j.1442-2906.2006.01272.x>.
- Xu, Z.L., 2008. Analysis on the indicator species and ecological groups of pelagic ostracods in the East China Sea. *Acta Oceanol. Sin.* 27, 83–93. <https://doi.org/10.1145/1360612.1360695>.
- Xu, Z.L., Gao, Q., 2011. Optimal salinity for dominant copepods in the East China Sea, determined using a yield density model. *Chin. J. Oceanol. Mar. Biol.* 29 (3), 514–523. <https://doi.org/10.1007/s00343-011-0090-y>.
- Xu, Z.L., Zhang, D., 2010. Yield-density model for determining optimal temperature and salinity for zooplankton: case studies with Appendicularia in the East China Sea. *Bull. Mar. Sci. Sci.* 86 (1), 149–164.
- Xue, Y., Guan, L., Tanaka, K., Ren, Y.P., 2017. Evaluating effects of rescaling and weighting data on habitat suitability modeling. *Fish. Res.* 188, 84–94. <https://doi.org/10.1016/j.fishres.2016.12.001>.
- Yabe, H., Takahashi, T., 1991. Factorized quasi-newton methods for nonlinear least squares problems. *Math. Program.* 51, 75–100. <https://doi.org/10.1007/BF01586927>.
- Yahuza, I., 2011. Yield-density equations and their application for agronomic research: a review. *Int. J. Biosci.* 1 (5), 1–17. <http://www.innspub.net/wp-content/uploads/2012/01/IJB-V1-No-5-p1-17.pdf>.
- Yen, K.W., Lu, H.J., Chang, Y., 2012. Using remote-sensing data to detect habitat suitability for yellowfin tuna in the Western and Central Pacific Ocean. *Int. J. Remote Sens.* 33, 7507–7522. <https://doi.org/10.1080/01431161.2012.685973>.
- Yu, W., Chen, X., Yi, Q., Chen, Y., Zhang, Y., 2015. Variability of suitable habitat of western winter-spring cohort for Neon flying Squid in the Northwest Pacific under anomalous environments. *PLoS One* 10 (4), 1–20. <https://doi.org/10.1371/journal.pone.0122997>.
- Yu, W., Yi, Q., Chen, X.J., Chen, Y., 2016. Modelling the effects of climate variability on habitat suitability of jumbo flying squid, *Dosidicus gigas*, in the Southeast Pacific Ocean off Peru. *ICES J. Mar. Sci.* 73, 239–250. <https://doi.org/10.1093/icesjms/fsv223>.